Few-Body Syst (2024) 65:29
https://doi.org/10.1007/s00601-024-01897-2

Tanja Kirchner · Wael Elkamhawy · Hans-Werner Hammer

Entanglement in Few-Nucleon Scattering Events

Received: 4 January 2024 / Accepted: 20 February 2024

Abstract We investigate the spin entanglement in few-nucleon scattering processes involving nucleons and deuterons. For this purpose, we consider the entanglement power introduced by Beane et al. We analyze different entanglement entropies as a basis to define the entanglement power of the strong interaction and calculate the corresponding entanglement powers for proton–neutron, neutron–deuteron, proton–deuteron, and deuteron–deuteron scattering. For the latter two processes, we also take into account the modification from the Coulomb interaction. In contrast to proton–neutron scattering, no universal low-energy features are evident in the spin entanglement in neutron–deuteron, proton–deuteron, and deuteron–deuteron scattering.

1 Introduction

Strongly interacting quantum systems can have universal properties that are independent of their interaction at short distances [1]. A well-known example is the low-energy scattering of bosons with large s-wave scattering length a and mass m. If a is positive and much larger than the range of the interaction R, there is a shallow two-body bound state with binding energy $B_2 = 1/(ma^2) + \mathcal{O}(R/a)$, and mean-square separation $a^2/2$. If a third particle is added, a three-body parameter, κ_*, is required to fully characterize the universal properties. For fixed a, this implies universal correlations between different three-body observables parameterized by κ_*, such as the Phillips line [2]. Moreover, the Efimov effect [3] generates a universal spectrum of three-body bound states characterized by a and κ_*.

Universality is also manifest in scattering observables. The scattering cross section of two particles at energy k^2/m, e.g., takes the universal form $d\sigma/d\Omega = 4a^2/(1+k^2a^2) + \mathcal{O}(R/a)$, and becomes scale invariant in the unitary limit of infinite scattering length. Similar universality relations exist for more bodies and more complicated systems of hadrons and nuclei with spin and isospin degrees of freedom (see Refs. [1,4–8] for more details). In few-nucleon systems, there is also an approximate Wigner $SU(4)$ symmetry that rotates the spin and isospin degrees of freedom into each other [9–11].

Methods from quantum information theory provide an alternative window on the universal properties of strongly interacting quantum systems. Beane et al. have shown that the suppression of spin entanglement in

T. Kirchner (✉) · W. Elkamhawy · H.-W. Hammer
Department of Physics, Institut für Kernphysik, Technische Universität Darmstadt, 64289 Darmstadt, Germany
E-mail: tkirchner@theorie.ikp.physik.tu-darmstadt.de

W. Elkamhawy
E-mail: elkamhawy@theorie.ikp.physik.tu-darmstadt.de

H.-W. Hammer
Helmholtz Forschungsakademie Hessen für FAIR (HFHF) and Extreme Matter Institute EMMI, GSI Helmholtzzentrum für Schwerionenforschung GmbH, 64291 Darmstadt, Germany
E-mail: Hans-Werner.Hammer@physik.tu-darmstadt.de

Published online: 22 March 2024

the S-matrix for nucleon–nucleon scattering is correlated with the Wigner $SU(4)$ spin–isospin symmetry [12]. Based on this observation, they have conjectured that dynamical entanglement suppression is a property of the strong interaction at low energies, giving rise to Wigner $SU(4)$ as an emergent symmetry. This idea was further elaborated in Ref. [13] and extended to systems of pions as well as pions and nucleons in Ref. [14]. Bai and Ren presented a formalism able to account for the Coulomb interaction using the screening method and investigated the entanglement entropy of p-^{3}He and n-^{3}H scattering [15].

In this work, we investigate the spin entanglement in the scattering of spin-1/2 and spin-1 particles with an application to proton–neutron, nucleon–deuteron, and deuteron–deuteron scattering processes in mind. We consider different entanglement entropies as a basis to define the entanglement power and investigate their universal low-energy properties. The entanglement of other degrees of freedom beyond spin is left for future work. The case of spin-1/2–spin-1/2 scattering based on the leading Taylor expansion of the von Neumann entropy was already investigated by Beane et al. [12]. The corresponding formalism for isospin-1/2–isospin-1 and isospin-1–isospin-1 scattering was discussed in [14]. We use our results to calculate the entanglement powers for proton–neutron, nucleon–deuteron, and deuteron–deuteron scattering. For the proton–neutron and deuteron–deuteron cases, the modification from the Coulomb interaction is also taken into account.

2 Formalism

We follow Ref. [12] and consider two particles that are initially uncorrelated. Thus, their spin state can be written as a product of the separate one-particle spin states $|\psi_{\rm in}\rangle = |\psi\rangle_1 \otimes |\psi\rangle_2$. We start by deriving a general initial state for spin-1/2 and spin-1 particles. Next, we analyze the correlation of the two spins induced by the scattering process. For this purpose, we define the scattering operator $\hat{S}$, i.e., the S-matrix, which transfers the initial state to the final scattered state

$$|\psi_{\rm out}\rangle = \hat{S}|\psi_{\rm in}\rangle. \tag{1}$$

The S-matrix is expressed in terms of the spin operators and the phase shifts in the corresponding spin channels.

The final state $|\psi_{\rm out}\rangle$ defines a density matrix $\hat{\rho} = |\psi_{\rm out}\rangle\langle\psi_{\rm out}|$ that contains all quantum-mechanical information about the state. To calculate correlations between the two final-state particles, we need the reduced density matrix for particle 1

$$\hat{\rho}_1 = {\rm Tr}_2[\hat{\rho}], \tag{2}$$

where particle 2 has been traced out. Note that the labels 1 and 2 are arbitrary and our results do not depend on this choice. For definiteness, however, we will always assume that particle 2 has been traced out in the following. Using the reduced density matrix, we can calculate entanglement entropies. These entropies quantify the degree of "entanglement" generated in the scattering process, which we will use as a measure of correlation between the two particles. These entropies will be shown in Sect. 2.3.

2.1 Initial State

For our calculations, we consider a general product state of the pure one-particle spin states. This implies that the two particles are initially uncorrelated. For the pure one-particle spin states, we take an arbitrary vector on the corresponding state manifold [16]. This will give us every possible spin state that generates a suitable density matrix that is Hermitian, positive semidefinite, normalized to trace one and is idempotent, i.e., $\hat{\rho}^2 = \hat{\rho}$. The spin states can be parameterized by a set of angles. In the following, we will discuss the general spin states for spin-1/2 and spin-1, as these are the cases we consider in our calculation.

Spin-1/2 For a spin-1/2 particle, we have two orthogonal spin states: $|1/2, 1/2\rangle$ and $|1/2, -1/2\rangle$. Therefore, two complex parameters (i.e., four real parameters) are required to specify a general pure state. By setting the overall phase and requiring the pure state to be properly normalized, two real parameters can be eliminated. The remaining two real parameters are angles that parameterize the corresponding complex manifold $\mathbf{CP}^1$ of all pure states (projective Hilbert space of complex dimension 1). This space is also known as the 2-sphere $\mathbf{S}^2$ or *Bloch sphere*, which is the unit sphere in three dimensions. It can be parameterized as [16]

$$|\psi_{S=1/2}\rangle = \cos\vartheta_1|1/2, 1/2\rangle + {\rm e}^{{\rm i}\nu_1}\sin\vartheta_1|1/2, -1/2\rangle, \tag{3}$$

where $0 < \vartheta_1 < \pi/2$ and $0 \leq \nu_1 < 2\pi$. The notion of distance of two points on $\mathbf{CP}^1$ is described by the *Fubini-Study metric*

$$\mathrm{d}s^2_{\mathrm{FS}}(\mathbf{CP}^1) = \mathrm{d}\vartheta_1^2 + \frac{1}{4}\sin^2(2\vartheta_1)\mathrm{d}\nu_1^2 \,. \tag{4}$$

Since we need to average over all possible initial states for the entanglement power defined in Ref. [12], we have to divide by the total volume of the corresponding manifold. In order to calculate the total volume of $\mathbf{CP}^1$, we require the differential *Fubini-Study volume element*

$$\mathrm{d}V_{\mathrm{FS}}(\mathbf{CP}^1) = \mathrm{d}\vartheta_1 \mathrm{d}\nu_1 \cos\vartheta_1 \sin\vartheta_1 \,. \tag{5}$$

Hence, the total volume reads

$$V_{\mathrm{FS}}(\mathbf{CP}^1) = \int \mathrm{d}V_{\mathrm{FS}}(\mathbf{CP}^1) = \pi \,. \tag{6}$$

Since $\mathbf{CP}^1$ is isomorphic to $\mathbf{S}^2$, one could also use standard spherical coordinates in three dimensions and parameterize all pure states on the Bloch sphere $\mathbf{S}^2$ as

$$|\psi_{S=1/2}\rangle = \cos\left(\frac{\vartheta}{2}\right)|1/2,\, 1/2\rangle + \mathrm{e}^{\mathrm{i}\phi}\sin\left(\frac{\vartheta}{2}\right)|1/2,\, -1/2\rangle \,. \tag{7}$$

Comparing the parameterizations in Eqs. (3) and (7), we find $\vartheta = 2\vartheta_1$ and $\phi = \nu_1$. The corresponding volume is 4π instead of π. However, averaging over all pure states will lead to the same results in either coordinates.

Spin-1 For spin-1, there are three basis states given by the spin projections $|1, -1\rangle$, $|1, 0\rangle$ and $|1, 1\rangle$. An arbitrary state can be parameterized by three complex parameters (i.e., six real parameters). Again, we eliminate two real parameters due to normalization and the overall phase. Therefore, we are left with four angles parameterizing the corresponding complex manifold $\mathbf{CP}^2$ of all pure states (projective Hilbert space of complex dimension 2). The resulting parameterization is given by [16]

$$|\psi_{S=1}\rangle = \cos\vartheta_1 \sin\vartheta_2 |1, -1\rangle + \mathrm{e}^{\mathrm{i}\nu_1}\sin\vartheta_1 \sin\vartheta_2 |1, 0\rangle + \mathrm{e}^{\mathrm{i}\nu_2}\cos\vartheta_2 |1, 1\rangle, \tag{8}$$

where $0 < \vartheta_1, \vartheta_2 < \pi/2$ and $0 \leq \nu_1, \nu_2 < 2\pi$. The differential volume element of the manifold is

$$\mathrm{d}V_{\mathrm{FS}}(\mathbf{CP}^2) = \mathrm{d}\vartheta_1\, \mathrm{d}\vartheta_2\, \mathrm{d}\nu_1\, \mathrm{d}\nu_2 \cos\vartheta_1 \cos\vartheta_2 \sin\vartheta_1 \sin^3\vartheta_2, \tag{9}$$

and integration gives us the total volume

$$V_{\mathrm{FS}}(\mathbf{CP}^2) = \int \mathrm{d}V_{\mathrm{FS}}(\mathbf{CP}^2) = \frac{\pi^2}{2} \,. \tag{10}$$

Note that the corresponding "generalized Bloch sphere" for spin-1 is much more intricate than for spin-1/2 and does not simply correspond to a unit sphere in 5 dimensions [16,17].

2.2 S-Matrix

Next, we derive a general expression for the scattering operator. We expand $\hat{S}$ in the identity matrix and powers of scalar products of the one-particle spin operators. We use this ansatz up to the square of the spin scalar product, as this is sufficient for spin-1/2 and spin-1 degrees of freedom,

$$\hat{S} = a\,\mathbb{1} + b\,\vec{S}_1 \cdot \vec{S}_2 + c\,(\vec{S}_1 \cdot \vec{S}_2)^2, \tag{11}$$

where $\mathbb{1}$ is defined as the tensor product of the identity operators for the first and the second particle, i.e., $\mathbb{1} = \mathbb{1}_1 \otimes \mathbb{1}_2$. Similarly, the spin scalar product is defined by $\vec{S}_1 \cdot \vec{S}_2 = \sum_i S_1^i \otimes S_2^i$, where the sum runs over all Cartesian components of the spin matrices for particle 1 and 2. We determine the parameters in Eq. (11) by demanding

$$\langle S = \alpha, M|\hat{S}|S = \alpha, M\rangle = e^{2i\delta_\alpha}, \tag{12}$$

for each spin channel α and all spin projections M. The scalar product of the spin matrices for particles 1 and 2 is expressed through squares of spin matrices in the usual way,

$$\vec{S}_1 \cdot \vec{S}_2 = \frac{1}{2}\left((\vec{S}_1 + \vec{S}_2)^2 - \vec{S}_1^2 - \vec{S}_2^2\right), \tag{13}$$

which can be evaluated straightforwardly using eigenvalue relations. A non-trivial check is given by the unitarity of $\hat{S}$. The condition $\hat{S}\hat{S}^\dagger = \hat{S}^\dagger\hat{S} = \mathbb{1}$ must hold true due to probability conservation.

Spin-1/2–spin-1/2 As a test of our procedure, we rederive the expression for $\hat{S}$ from [12] for the s-wave scattering of spin-1/2 nucleons. There are two spin channels, $S = 0$ and $S = 1$, with phase shifts δ_0 and δ_1, respectively. The ansatz from above leads to the scattering operator

$$\hat{S}_{\frac{1}{2}\frac{1}{2}} = \frac{1}{4}\left(\mathrm{e}^{2\mathrm{i}\delta_0} + 3\mathrm{e}^{2\mathrm{i}\delta_1}\right)\mathbb{1} - \left(\mathrm{e}^{2\mathrm{i}\delta_0} - \mathrm{e}^{2\mathrm{i}\delta_1}\right)\vec{S}_1 \cdot \vec{S}_2, \tag{14}$$

in agreement with the expression given in [12].

Spin-1–spin-1/2 In the s-wave scattering of a spin-1 and spin-1/2 particle, we have the two spin channels $S = 1/2$ and $S = 3/2$ with phase shifts $\delta_{1/2}$ and $\delta_{3/2}$, respectively. Using the strategy described above, the scattering operator is found to be

$$\hat{S}_{1\frac{1}{2}} = \frac{1}{3}\left(\mathrm{e}^{2\mathrm{i}\delta_{1/2}} + 2\mathrm{e}^{2\mathrm{i}\delta_{3/2}}\right)\mathbb{1} - \frac{2}{3}\left(\mathrm{e}^{2\mathrm{i}\delta_{1/2}} - \mathrm{e}^{2\mathrm{i}\delta_{3/2}}\right)\vec{S}_1 \cdot \vec{S}_2, \tag{15}$$

which agrees with the results obtained in [14] for the πN system when spin and isospin are exchanged.

Spin-1–spin-1 For s-wave spin-1–spin-1 scattering, the total spins $S = 0$, $S = 1$, and $S = 2$ are possible. The general form of the scattering operator for distinguishable particles is given by

$$\begin{aligned}\hat{S}_{11} = &-\frac{1}{3}\left(\mathrm{e}^{2\mathrm{i}\delta_0} - 3\mathrm{e}^{2\mathrm{i}\delta_1} - \mathrm{e}^{2\mathrm{i}\delta_2}\right)\mathbb{1} - \frac{1}{2}\left(\mathrm{e}^{2\mathrm{i}\delta_1} - \mathrm{e}^{2\mathrm{i}\delta_2}\right)\vec{S}_1 \cdot \vec{S}_2 \\ &+ \left(\frac{1}{3}\mathrm{e}^{2\mathrm{i}\delta_0} - \frac{1}{2}\mathrm{e}^{2\mathrm{i}\delta_1} + \frac{1}{6}\mathrm{e}^{2\mathrm{i}\delta_2}\right)(\vec{S}_1 \cdot \vec{S}_2)^2,\end{aligned} \tag{16}$$

with the corresponding phase shifts δ_0, δ_1, and δ_2. Here, all three operators appearing in Eq. (11) contribute. The equivalent result for isospin degrees of freedom was given in [14] considering the case of $\pi\pi$ scattering.

For s-wave scattering of two identical bosons with spin-1, only wave functions symmetric under particle exchange are allowed by Bose statistics. Thus, only the total spins $S = 0$ and $S = 2$ are allowed. The $S = 1$ state is forbidden by symmetry, i.e., neither interaction nor free propagation is allowed in this channel. Therefore, we construct an S-matrix that is unitary in the $S = 0$ and $S = 2$ channel but identically zero in the $S = 1$ channel. This S-matrix can be obtained from Eq. (16) by replacing $\mathrm{e}^{2\mathrm{i}\delta_1} \to 0$, which leads to the scattering operator

$$\begin{aligned}\hat{S}_{dd} = &-\frac{1}{3}\left(\mathrm{e}^{2\mathrm{i}\delta_0} - \mathrm{e}^{2\mathrm{i}\delta_2}\right)\mathbb{1} + \frac{1}{2}\mathrm{e}^{2\mathrm{i}\delta_2}\,\vec{S}_1 \cdot \vec{S}_2 \\ &+ \frac{1}{6}\left(2\mathrm{e}^{2\mathrm{i}\delta_0} + \mathrm{e}^{2\mathrm{i}\delta_2}\right)(\vec{S}_1 \cdot \vec{S}_2)^2\,.\end{aligned} \tag{17}$$

Formally, this corresponds to applying a projection operator $\hat{P}$ to S_{11} which projects the S-matrix on the subspace with $S = 0, 2$,

$$\hat{S}_{dd} = \hat{P}^\dagger \hat{S}_{11} \hat{P}\,. \tag{18}$$

Alternatively, the operator $\hat{P}$ can also act on the initial product state $|\psi_{\mathrm{in}}\rangle$ in Eq. (1), leading to the same result for the entanglement entropy. We will come back to this viewpoint below when we discuss the entanglement power for dd scattering.

2.3 Entropies

To quantify the correlation between the two spins after the scattering process, we use entropies as a measure of the entanglement. We examine different entropy definitions as a basis for the entanglement power and investigate whether they are equally suitable to describe the generated entanglement.

First, we consider the standard von Neumann entropy

$$E_N(\hat{\rho}_1) = -\mathrm{Tr}[\hat{\rho}_1 \ln(\hat{\rho}_1)] = -\sum_i \lambda_i \ln(\lambda_i), \tag{19}$$

where the λ_i with $i = 1, 2, \ldots$ denote the eigenvalues of the reduced density matrix $\hat{\rho}_1$. Since the calculation of the von Neumann entropy requires the diagonalization of the density matrix, it is often convenient to study the Taylor expansions of the von Neumann entropy of order n,

$$E_n(\hat{\rho}_1) = -\mathrm{Tr}\left[\hat{\rho}_1 \sum_{j=1}^{n} \frac{(-1)^{j+1}\,(\hat{\rho}_1 - \mathbb{1})^j}{j}\right]. \tag{20}$$

Finally, we also investigate the Rényi entropies

$$E_R(\hat{\rho}_1, \alpha) = \frac{1}{1-\alpha} \ln\left(\mathrm{Tr}[\hat{\rho}_1^{\alpha}]\right), \qquad \alpha > 0, \tag{21}$$

$$= \frac{1}{1-\alpha} \ln\left(\sum_i \lambda_i^{\alpha}\right), \tag{22}$$

for $\alpha = 0.5$ and $\alpha = 2$. Note that in the limit $\alpha \to 1$, the Rényi entropy tends to the von Neumann entropy.

2.4 Averaging Over Initial States: Entanglement Power

Following [12], the "entanglement power" of the S-Matrix is defined by calculating the entropy E of particle 1 for a reduced density matrix $\hat{\rho}_1 = \mathrm{Tr}_2[\hat{\rho}]$, and averaging the entropy E over all possible initial states of the scattering process, meaning

$$\epsilon = \frac{1}{V_{\mathrm{FS}(1)} V_{\mathrm{FS}(2)}} \int \mathrm{d}V_{\mathrm{FS}(1)} \mathrm{d}V_{\mathrm{FS}(2)}\, E, \tag{23}$$

where $\mathrm{d}V_{\mathrm{FS}(1)}$ and $\mathrm{d}V_{\mathrm{FS}(2)}$ denote the Fubini-Study volume elements for particle 1 and 2, respectively. This average cancels out the dependence on the initial state. For the leading Taylor expansion of the von Neumann entropy and spin-$1/2$ particles, this reduces to the definition of Ref. [12],

$$\epsilon = 1 - \frac{1}{16\pi^2} \int \mathrm{d}\Omega_1 \mathrm{d}\Omega_2 \mathrm{Tr}_1[\hat{\rho}_1^2]\,. \tag{24}$$

Next, we revisit the case of nucleon–nucleon scattering and apply our results to experimental data for nucleon–deuteron and deuteron–deuteron scattering.

3 Application to Nuclear Scattering Processes

3.1 Neutron–Proton Scattering

We start with the case of neutron–proton scattering, which was already discussed in [12] for the entanglement power based on the leading Taylor expansion of the von Neumann entropy. Using the form of the S-matrix, Eq. (14), and the expressions in Sect. 2.3, the entanglement powers can be calculated from the scattering phase shifts. Since we are interested in scattering close to threshold, we focus on the s-wave contribution.

The Taylor expansions E_n of the Neumann entropy as function of the reduced density matrix $\hat{\rho}$, Eq. (20), up to order $n = 7$ are listed in Table 1. Their calculation does not require the diagonalization of the density matrix. Analytic expressions for the s-wave contribution to the corresponding entanglement powers ϵ_n in terms of the spin-singlet and spin-triplet phase shifts δ_0 and δ_1 are therefore straightforward to calculate. Inserting the general form of the S-matrix, Eq. (14), we obtain the expressions for ϵ_n given in Table 2. The entanglement powers based on the von Neumann entropy, ϵ_N, and Rényi entropies, ϵ_R, are calculated numerically.

The entanglement powers can be evaluated using the Nijmegen partial wave analysis PWA93 [18,19]. Other potential models have been evaluated in [12] and lead to similar results. The evaluation of the entanglement powers based on the Taylor-expanded von Neumann entropy, ϵ_n for $n = 1, 3, 5, 7$, with phase shift data from the Nijmegen partial wave analysis PWA93 [18,19] are shown in the left plot of Fig. 1. In the right panel, we show a comparison of ϵ_1 with the entanglement power based on the full von Neumann entropy, ϵ_N, and the Rényi entropies ϵ_R for $\alpha = 0.5$ and $\alpha = 2$. Evidently, the qualitative behavior of all entanglement powers is

Table 1 Taylor expansions E_n of the von Neumann entropy E_N as function of the reduced density matrix $\hat{\rho}$ up to order $n = 7$

n	E_n
1	$1 - \mathrm{Tr}[\hat{\rho}^2]$
2	$\frac{3}{2} - 2\mathrm{Tr}[\hat{\rho}^2] + \frac{1}{2}\mathrm{Tr}[\hat{\rho}^3]$
3	$\frac{11}{6} - 3\mathrm{Tr}[\hat{\rho}^2] + \frac{3}{2}\mathrm{Tr}[\hat{\rho}^3] - \frac{1}{3}\mathrm{Tr}[\hat{\rho}^4]$
4	$\frac{25}{12} - 4\mathrm{Tr}[\hat{\rho}^2] + 3\mathrm{Tr}[\hat{\rho}^3] - \frac{4}{3}\mathrm{Tr}[\hat{\rho}^4] + \frac{1}{4}\mathrm{Tr}[\hat{\rho}^5]$
5	$\frac{137}{60} - 5\mathrm{Tr}[\hat{\rho}^2] + 5\mathrm{Tr}[\hat{\rho}^3] - \frac{10}{3}\mathrm{Tr}[\hat{\rho}^4] + \frac{5}{4}\mathrm{Tr}[\hat{\rho}^5] - \frac{1}{5}\mathrm{Tr}[\hat{\rho}^6]$
6	$\frac{49}{20} - 6\mathrm{Tr}[\hat{\rho}^2] + \frac{15}{2}\mathrm{Tr}[\hat{\rho}^3] - \frac{20}{3}\mathrm{Tr}[\hat{\rho}^4] + \frac{15}{4}\mathrm{Tr}[\hat{\rho}^5] - \frac{6}{5}\mathrm{Tr}[\hat{\rho}^6] + \frac{1}{6}\mathrm{Tr}[\hat{\rho}^7]$
7	$\frac{363}{140} - 7\mathrm{Tr}[\hat{\rho}^2] + \frac{21}{2}\mathrm{Tr}[\hat{\rho}^3] - \frac{35}{3}\mathrm{Tr}[\hat{\rho}^4] + \frac{35}{4}\mathrm{Tr}[\hat{\rho}^5] - \frac{21}{5}\mathrm{Tr}[\hat{\rho}^6] + \frac{7}{6}\mathrm{Tr}[\hat{\rho}^7] - \frac{1}{7}\mathrm{Tr}[\hat{\rho}^8]$

Table 2 s-wave scattering contributions to the entanglement powers ϵ_n based on Taylor expansions E_n of the von Neumann entropy E_N for $n = 1 \ldots 7$ expressed through the spin-singlet and spin-triplet phase shifts δ_0 and δ_1

n	ϵ_n
1	$\frac{1}{6}\sin[2(\delta_0 - \delta_1)]^2$
2	$\frac{5}{24}\sin[2(\delta_0 - \delta_1)]^2$
3	$\frac{1}{720}(167 + 3\cos[4(\delta_0 - \delta_1)])\sin[2(\delta_0 - \delta_1)]^2$
4	$\frac{1}{5760}(1429 + 51\cos[4(\delta_0 - \delta_1)])\sin[2(\delta_0 - \delta_1)]^2$
5	$\frac{1}{403200}(104869 + 5406\cos[4(\delta_0 - \delta_1)] + 45\cos[8(\delta_0 - \delta_1)])\sin[2(\delta_0 - \delta_1)]^2$
6	$\frac{1}{537600}(144867 + 9508\cos[4(\delta_0 - \delta_1)] + 185\cos[8(\delta_0 - \delta_1)])\sin[2(\delta_0 - \delta_1)]^2$
7	$\frac{1}{45158400}(12511358 + 978417\cos[4(\delta_0 - \delta_1)] + 30690\cos[8(\delta_0 - \delta_1)]$ $+175\cos[12(\delta_0 - \delta_1)])\sin[2(\delta_0 - \delta_1)]^2$

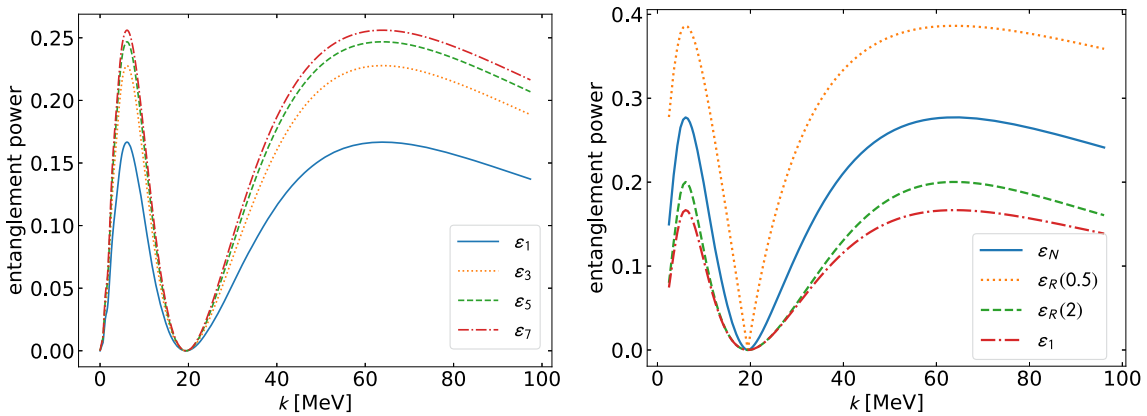

Fig. 1 Comparison of the different entanglement powers as a function of the relative momentum k evaluated using phase shift data from the Nijmegen partial wave analysis PWA93 [18,19] for pn scattering. Left panel: using different Taylor expansions of the von Neumann entropy: $\epsilon_i, i = 1, 3, 5, 7$. Right panel: using the von Neumann entropy ϵ_N and Rényi entropies ϵ_R for $\alpha = 0.5$ and $\alpha = 2$ compared to ϵ_1

the same, they are just scaled differently. In particular, the position of minima and maxima stays the same. Thus, all definitions carry the same physical information. We observe that the difference between neighboring Taylor expansions ϵ_n decreases with n. This suggests that the expansion in Eq. (20) converges for pn scattering and all entanglement powers are equally suited to describe the entanglement created in the scattering process. Thus, our study confirms the results of Ref. [12] for the pn case, including the evidence for an emergent Wigner $SU(4)$ symmetry.

3.2 Phenomenology

The qualitative behavior in the *pn* case can also be understood based on the effective range expansion of the phase shifts,

$$k \cot \delta_j(k) = -\frac{1}{a_j} + \frac{r_j}{2}k^2 + \ldots, \quad j = 0, 1, \tag{25}$$

where k is the relative momentum and the total energy in the center of mass frame is k^2/m. Moreover, a_j and r_j are the scattering length and effective range in the spin channel j, respectively.

Since, in our case, the scattering lengths are large, we can neglect effective range effects at low energies, $kr_j \ll 1$, and the phase shifts can be approximated by $\delta_j(k) = \operatorname{arccot}(-1/(a_j k))$. Inserting this expression for both channels in the entanglement power ϵ_1 from Table 2 gives us [20]

$$\epsilon_1 = \frac{2}{3}\frac{(a_1 - a_0)^2 k^2 \left(1 + a_0 a_1 k^2\right)^2}{\left(1 + a_0^2 k^2\right)^2 \left(1 + a_1^2 k^2\right)^2}, \tag{26}$$

which allows us to determine the minima and maxima analytically. The minima of ϵ_1 are at $k_{\min,1} = 0$ MeV and $k_{\min,2} = (-a_1 a_0)^{-1/2}$, while the maxima are given by

$$k_{\max,\pm} = \frac{\pm(a_0 - a_1) - \sqrt{a_0^2 - 6a_0 a_1 + a_1^2}}{2a_0 a_1}. \tag{27}$$

Using the explicit values $a_0 = 5\,\text{fm}$ and $a_1 = -20\,\text{fm}$ gives the minima at $k_{\min,1} = 0$ MeV and $k_{\min,2} \approx 20\,\text{MeV}$ and the maxima at $k_{\max,+} \approx 7\,\text{MeV}$ and $k_{\max,-} \approx 57\,\text{MeV}$. This agrees well with the full numerical results shown in Fig. 1.

4 *nd* and *pd* Scattering

Restricting ourselves to s-wave scattering, the nucleon and the deuteron can scatter in the ${}^2S_{1/2}$ and ${}^4S_{3/2}$ channels. The general form of the scattering matrix for this case is given in Eq. (15).

4.1 Coulomb Interaction

In the *pd* case, we also need to take into account the Coulomb interaction between the proton and the deuteron. The s-wave phase shifts in presence of a strong interaction and a Coulomb interaction split up into three pieces,

$$\delta_{\text{tot}}(k) = -\eta_k \log(2kr) + \sigma(k) + \delta_N(k), \tag{28}$$

a logarithmic part, a pure Coulomb part σ, and a Coulomb-modified nuclear part δ_N (also known as Coulomb-subtracted phase shift), see, e.g., Refs. [21,22]. Here, δ_N is the additional strong phase shift relative to the Coulomb wave function while the pure s-wave Coulomb phase shift σ is given by $\sigma(k) = \arg\Gamma(1 + i\eta_k)$. Moreover, $\eta_k = \alpha_e Z_1 Z_2 \mu / k$ is the Sommerfeld parameter, k is the relative momentum of the scattered particles, $\alpha_e = e^2/(4\pi)$ is the electromagnetic fine structure constant in Heaviside-Lorentz units, μ is their reduced mass, and the Z_i are their charge numbers. Defining the Coulomb momentum scale $k_c = \alpha_e Z_1 Z_2 \mu$, the Sommerfeld parameter can also be written as $\eta_k = k_c/k$. The amplitude describing the effects of the strong force relative to the Coulomb interaction takes the form

$$f_{SC}(k) = \frac{e^{2i\sigma(k)}}{k \cot \delta_N(k) - ik}, \tag{29}$$

where the pure Coulomb phase shift enters as a prefactor. We can set up our scattering matrix the same way as before, but this time with the Coulomb-subtracted phase shift δ_N. We emphasize that δ_N is defined relative to the outgoing Coulomb waves instead of plane waves as in the case without Coulomb.

We will see below that the entanglement entropies for *pd* scattering only depend on the difference of the s-wave phase shifts $\delta_{1/2}$ and $\delta_{3/2}$. Thus, our procedure can be justified by considering screened Coulomb

Table 3 s-wave scattering contributions to the entanglement powers ϵ_n based on Taylor expansions E_n of the von Neumann entropy E_N for $n = 1, 2$ expressed through the spin-doublet and spin-quartet phase shifts $\delta_{1/2}$ and $\delta_{3/2}$

n	ϵ_n
1	$\frac{8}{243}(17 + 10\cos[2(\delta_{1/2} - \delta_{3/2})])\sin[\delta_{1/2} - \delta_{3/2}]^2$
2	$\frac{10}{243}(17 + 10\cos[2(\delta_{1/2} - \delta_{3/2})])\sin[\delta_{1/2} - \delta_{3/2}]^2$

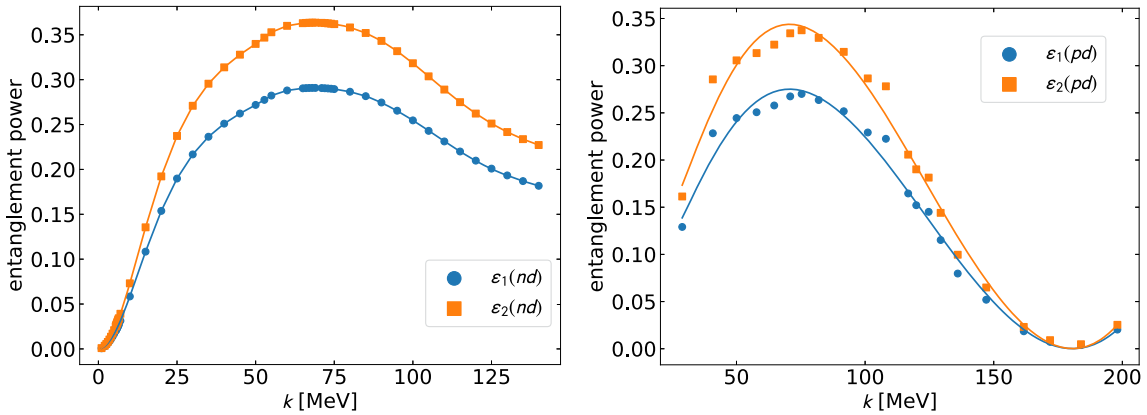

Fig. 2 Comparison of the entanglement powers ϵ_1 and ϵ_2 for nd and pd scattering based on the Taylor expansions of the von Neumann entropy. Left panel: nd scattering with phase shifts from the pionless effective field theory calculation of Vanasse [23]. Right panel: pd scattering based on phase shifts obtained from experimental data analyzed in Ref. [24]. In both plots the data are represented by points while the curves are inserted to guide the eye

potentials as in Ref. [15]. The contribution from the first two terms in Eq. (28) will simply cancel out in the entanglement entropy, such that the screening can safely be removed. As a consequence, the effect of Coulomb interaction on the entanglement enters only via the Coulomb-modified nuclear part δ_N. It can only be observed in the difference between nd and pd scattering data. This result is not unexpected since the Coulomb interaction is spin-independent and thus cannot create any spin entanglement.

4.2 Results

We have calculated analytical expressions for the entanglement power based on the first two Taylor expansions of the von Neumann entropy. They are given in Table 3. The result for the first Taylor expansion, ϵ_1, agrees with the entanglement entropy obtained in [14] for πN scattering. The entanglement powers based on the von Neumann entropy, ϵ_N, and Rényi entropies, ϵ_R, for $\alpha = 0.5$ and $\alpha = 2$ will be calculated numerically as before. One can already see that the two expansions only differ by a constant rescaling. Evaluating these expressions for nd and pd scattering data gives us the left and right plot in Fig. 2, respectively. As discussed above, only the Coulomb-modified nuclear phase shift δ_N contributes while the pure Coulomb contribution, which is the same in both spin channels, cancels out. In the left panel, we compare ϵ_1 and ϵ_2 for nd scattering using phase shifts from the pionless effective field theory calculation of Vanasse [23]. In the right panel, we show the corresponding results for pd scattering based on phase shifts obtained from experimental data analyzed in Ref. [24]. Both plots show similar qualitative behavior with a minimum at relatively high momenta of order 150 MeV. This minimum is not expected to be governed by universal low-energy physics.

Figure 3 shows the comparison of entanglement powers for nd scattering based on different entropies as discussed in the caption. As in the nucleon-nucleon case, the qualitative features are very similar such that the much easier to calculate entanglement powers ϵ_1 and ϵ_2 are sufficient for our purposes. Note also that no characteristic signature of the triton virtual state below the scattering threshold [25–27] can be seen since the entanglement power vanishes at $k = 0$.

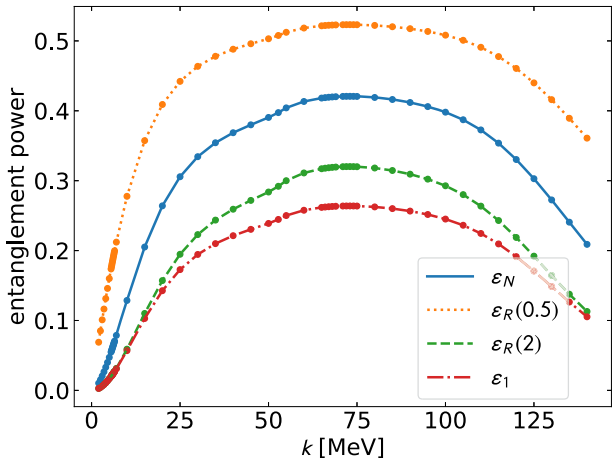

Fig. 3 Comparison of the entanglement powers for nd scattering based on the von Neumann entropy, ϵ_N, and Rényi entropies, ϵ_R, for $\alpha = 0.5$ and $\alpha = 2$ with ϵ_1. Phase shifts are taken from the pionless effective field theory calculation of Vanasse [23]. The data are represented by points. The lines are added to guide the eye

4.3 Phenomenology

Inserting the effective range expansion for s-waves given in Eq. (25) for the doublet and quartet nd channels into the analytical expression for ϵ_1 from Table 3 allows for a discussion of the qualitative features in the nd case based on effective range parameters. Keeping only the scattering length contribution to the phase shifts, we obtain

$$\epsilon_1 = \frac{8}{243}\left(17 + 10\frac{1-\left(a_{1/2}^2 - 4a_{1/2}a_{3/2} + a_{3/2}^2\right)k^2 + a_{1/2}^2 a_{3/2}^2 k^4}{\left(1+a_{1/2}^2k^2\right)\left(1+a_{3/2}^2k^2\right)}\right) \times \frac{\left(a_{1/2}-a_{3/2}\right)^2 k^2}{\left(1+a_{1/2}^2k^2\right)\left(1+a_{3/2}^2k^2\right)}. \tag{30}$$

There are no minima apart from $k_{\min} = 0$ within the range of applicabilty of the scattering length approximation. This is in agreement with the full numerical results shown in Fig. 2 despite the very limited range of applicability of the scattering length approximation in nucleon–deuteron scattering.

The range of applicability can be extended by including the effective range term in the quartet channel and using a modified effective range expansion for the doublet channel which includes a pole in $k \cot \delta_{1/2}(k)$ at negative energies related to the triton virtual state (see, e.g., Refs. [27–29]). The corresponding expression for ϵ_1 can reproduce the entanglement power for nd scattering in Fig. 2 up to the maximum at $k \approx 75$ MeV. We refrain from showing the explicit formula for this case since it is cumbersome and does not offer any deeper insights.

5 dd Scattering

The general form of the scattering matrix for s-wave dd scattering is given in Eq. (17). Due to the Bose symmetry of the two-deuteron state, only the $S = 0$ and $S = 2$ channels are present.

5.1 Results

Because the $(\vec{S}_1 \cdot \vec{S}_2)^2$ operator contributes, the dd S-matrix is more complicated than in the previous cases and the evaluation of the entanglement entropy is computationally more expensive. Since our investigations above demonstrate that all entanglement entropies are equally suitable for our purpose, we focus on the leading Taylor expansion of the von Neumann entropy in the dd case. The analytical expression for ϵ_1 is given in Table 4. We give the result for s-wave dd scattering based on Eq. (17) and, for completeness, the general result

Table 4 s-wave scattering contributions to the entanglement power ϵ_1 for dd scattering expressed through the phase shifts δ_0 and δ_2 for $S = 0$ and $S = 2$ (first system). The general result including δ_1 for the $S = 1$ channel applies to the second system of distinguishable particles

system	ϵ_1
dd	$\frac{1}{576}(153 - 70\cos[2(\delta_0 - \delta_2)] - 20\cos[4(\delta_0 - \delta_2)])$
distinguishable particles	$\frac{1}{648}\Big(156 - 6\cos[4(\delta_0 - \delta_1)] - 65\cos[2(\delta_0 - \delta_2)] - 10\cos[4(\delta_0 - \delta_2)]$ $-60\cos[4(\delta_1 - \delta_2)] - 15\cos(2[\delta_0 - 2\delta_1 + \delta_2])\Big)$

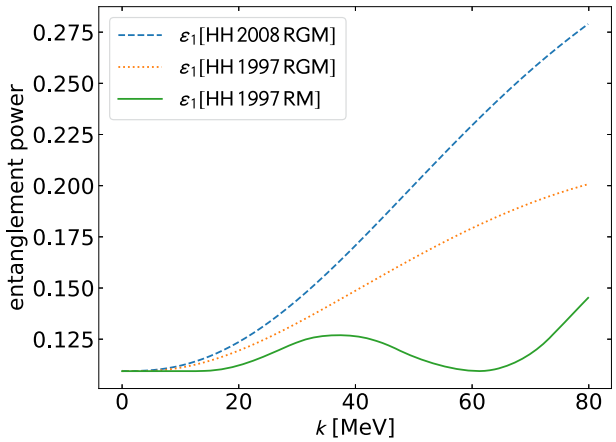

Fig. 4 Entanglement power ϵ_1 for dd scattering phase shifts obtained by Hofmann and Hale. The solid line is based on the R-matrix analysis of Ref. [30]. The dashed and dotted lines are calculated using the resonating group model (RGM) calculations for the AV18 + Urbana-IX and Bonn potentials from Refs. [30] and [31], respectively

including δ_1 for s-wave scattering of distinguishable spin-1 particles based on Eq. (16). In the dd case, the entanglement power starts with a non-zero value at $k = 0$. This can be understood from the structure of the spin-projected initial state $\hat{P}|\psi_{\rm in}\rangle$. The initial product state $|\psi_{\rm in}\rangle$ contains all spins. Applying $\hat{P}$ from Eq. (18) to project on the $S = 0, 2$ components, however, creates an entangled state. As a consequence, the initial state has a non-vanishing entanglement entropy, which leads to an offset in the entanglement power. For the discussion of universal features of the entanglement created in the scattering process, only the relative maxima and minima of ϵ_1 are relevant. In both cases, dd scattering and distinguishable particles, the entanglement power depends only on the difference of phase shifts for different total spins S. For dd scattering, the pure Coulomb contribution thus cancels out in the entanglement power.[1] As a consequence, the entanglement power for s-wave dd scattering is determined by the Coulomb-modified strong phase shift alone, similar to the pd case.

Next, we evaluate the entanglement power using the Coulomb-modified dd phase shifts obtained by Hofmann and Hale [30,31]. In Ref. [30], they presented a calculation of dd scattering in the resonating group model (RGM) for the Bonn potential and compared to a charge-independent, Coulomb corrected R-matrix analysis of reaction data in the four-nucleon system. This work was updated in Ref. [31] with an RGM calculation using the AV18 two-nucleon potential and an Urbana-IX three-nucleon force and a new R-matrix analysis. As in the previous section, we evaluate the entanglement power ϵ_1 using the Coulomb-modified nuclear phase shifts. In Fig. 4, we show the corresponding results for ϵ_1.

While the entanglement powers shown in Fig. 4 agree at low momenta up to about 10 MeV, there are significant differences at higher momenta. The RGM calculations for both potentials show a monotonic increase of ϵ_1, but differ in their absolute size at larger momenta. No universal features are evident. The R-matrix analysis from Ref. [30], however, shows a minimum of the entanglement power around $k = 60$ MeV. The significance of this feature and the reason for its absence in the RGM calculations deserve further study.

[1] Note that this cancellation would not occur in dd scattering if Eq. (16) with $\delta_1 = 0$ was used for the S-Matrix instead of Eq. (17). In this case, the corresponding entanglement power would depend on the screening radius for the Coulomb potential and the screening could not be removed at the end of the calculation.

Moreover, it would be interesting to investigate the entanglement power in the threshold region more closely. This will shed some light on the signature of the ^{4}He excited state slightly above the scattering threshold in the entanglement power [32,33]. The exact location of this resonance has received some recent interest in the context of investigations of the monopole transition form factor of the ^{4}He nucleus [34–36].

6 Summary

In this paper, we have investigated the spin entanglement in few-nucleon scattering processes involving nucleons and deuterons using the entanglement power introduced by Beane et al. [12]. We have considered different entanglement entropies as a basis for the calculation of the entanglement power for the cases of spin-$1/2$–spin-$1/2$, spin-$1/2$–spin-1 and spin-1–spin-1 scattering. The entanglement powers were evaluated for neutron–proton, neutron–deuteron, proton–deuteron, and deuteron–deuteron scattering, taking into account the Coulomb contribution for the latter two processes. For all systems considered, the different entropies give the same information about the entanglement and are therefore equally well suited for quantifying these properties. In practice, it is preferable to use the original entanglement power defined in Ref. [12] based on the first order Taylor expansion of the von Neumann entropy. While the linear approximation may in principle miss information if the reduced density matrix is not close to the unit operator, this was not found to be the case for the considered processes. In all considered cases, the entanglement power for s-wave scattering only depends on the difference of phase shifts for different spin channels. For charged particles, the pure Coulomb contribution thus cancels out and the entanglement power is determined by the Coulomb-modified strong phase shift alone.

Finally, no universal low-energy features in the entanglement powers for neutron–deuteron and proton–deuteron scattering could be identified. The deuteron–deuteron case deserves further study both in the threshold region where the ^{4}He excited state resides and at intermediate momenta. In the future, it would be interesting to go beyond pure spin entanglement and investigate the possible manifestation of large-scattering-length universality in the spatial entanglement of light nuclear systems.

Acknowledgements We thank Jared Vanasse for sharing the results of his pionless effective field theory calculations of neutron–deuteron scattering and Matthias Göbel for constructive comments. This work was supported by the Deutsche Forschungsgemeinschaft (DFG, German Research Foundation)–Projektnummer 279384907—SFB 1245 and by the German Federal Ministry of Education and Research (BMBF) (Grant No. 05P21RDFNB).

Author Contributions H-WH designed the research project. TK and WE carried out the calculations. TK prepared the figures. TK, WE, and H-WH wrote the manuscript.

Data Availability No datasets were generated or analysed during the current study.

Declarations

Conflict of interest The authors declare no conflict of interest.

References

1. E. Braaten, H.W. Hammer, Universality in few-body systems with large scattering length. Phys. Rep. **428**, 259–390 (2006). https://doi.org/10.1016/j.physrep.2006.03.001. arXiv:cond-mat/0410417
2. A.C. Phillips, Consistency of the low-energy three-nucleon observables and the separable interaction model. Nucl. Phys. A **107**, 209–216 (1968). https://doi.org/10.1016/0375-9474(68)90737-9
3. V. Efimov, Energy levels arising form the resonant two-body forces in a three-body system. Phys. Lett. B **33**, 563–564 (1970). https://doi.org/10.1016/0370-2693(70)90349-7
4. E. Epelbaum, H.-W. Hammer, U.-G. Meissner, Modern theory of nuclear forces. Rev. Mod. Phys. **81**, 1773–1825 (2009). https://doi.org/10.1103/RevModPhys.81.1773. arXiv:0811.1338
5. T. Frederico, A. Delfino, L. Tomio, M.T. Yamashita, Universal aspects of light halo nuclei. Prog. Part. Nucl. Phys. **67**, 939–994 (2012). https://doi.org/10.1016/j.ppnp.2012.06.001

6. H.W. Hammer, C. Ji, D.R. Phillips, Effective field theory description of halo nuclei. J. Phys. G **44**(10), 103002 (2017). https://doi.org/10.1088/1361-6471/aa83db. arXiv:1702.08605
7. H.W. Hammer, S. König, U. van Kolck, Nuclear effective field theory: status and perspectives. Rev. Mod. Phys. **92**(2), 025004 (2020). https://doi.org/10.1103/RevModPhys.92.025004. arXiv:1906.12122
8. A. Kievsky, L. Girlanda, M. Gattobigio, M. Viviani, Efimov physics and connections to nuclear physics. Ann. Rev. Nucl. Part. Sci. **71**, 465–490 (2021). https://doi.org/10.1146/annurev-nucl-102419-032845. arXiv:2102.13504
9. T. Mehen, I.W. Stewart, M.B. Wise, Wigner symmetry in the limit of large scattering lengths. Phys. Rev. Lett. **83**, 931–934 (1999). https://doi.org/10.1103/PhysRevLett.83.931. arXiv:hep-ph/9902370
10. P.F. Bedaque, H.W. Hammer, U. van Kolck, Effective theory of the triton. Nucl. Phys. A **676**, 357–370 (2000). https://doi.org/10.1016/S0375-9474(00)00205-0. arXiv:nucl-th/9906032
11. J. Vanasse, D.R. Phillips, Three-nucleon bound states and the Wigner-SU(4) limit. Few Body Syst. **58**(2), 26 (2017). https://doi.org/10.1007/s00601-016-1173-2. arXiv:1607.08585
12. S.R. Beane, D.B. Kaplan, N. Klco, M.J. Savage, Entanglement suppression and emergent symmetries of strong interactions. Phys. Rev. Lett. **122**(10), 102001 (2019). https://doi.org/10.1103/PhysRevLett.122.102001. arXiv:1812.03138
13. I. Low, T. Mehen, Symmetry from entanglement suppression. Phys. Rev. D **104**(7), 074014 (2021). https://doi.org/10.1103/PhysRevD.104.074014. arXiv:2104.10835
14. S.R. Beane, R.C. Farrell, M. Varma, Entanglement minimization in hadronic scattering with pions. Int. J. Mod. Phys. A **36**(30), 2150205 (2021). https://doi.org/10.1142/S0217751X21502055. arXiv:2108.00646
15. D. Bai, Z. Ren, Entanglement generation in few-nucleon scattering. Phys. Rev. C **106**(6), 064005 (2022). https://doi.org/10.1103/PhysRevC.106.064005. arXiv:2212.11092
16. I. Bengtsson, K. Zyczkowski, *Geometry of Quantum States: An Introduction to Quantum Entanglement* (Cambridge University Press, Cambridge, 2006). https://doi.org/10.1017/CBO9780511535048
17. S.K. Goyal, B.N. Simon, R. Singh, S. Simon, Geometry of the generalized Bloch sphere for qutrits. J. Phys. A **49**(16), 165203 (2016). https://doi.org/10.1088/1751-8113/49/16/165203. arXiv:1111.4427
18. V.G.J. Stoks, R.A.M. Klomp, M.C.M. Rentmeester, J.J. de Swart, Partial wave analysis of all nucleon–nucleon scattering data below 350-MeV. Phys. Rev. C **48**, 792–815 (1993). https://doi.org/10.1103/PhysRevC.48.792
19. R.U. Nijmegen, *NN-Online*, http://nn-online.org/ (2005)
20. S.R. Beane, R.C. Farrell, Geometry and entanglement in the scattering matrix. Ann. Phys. **433**, 168581 (2021). https://doi.org/10.1016/j.aop.2021.168581. arXiv:2011.01278,
21. J.R. Taylor, *Scattering Theory: The Quantum Theory of Nonrelativistic Collisions* (Wiley, New York, 1972)
22. R. Higa, G. Rupak, A. Vaghani, Radiative ^{3}He$(\alpha, \gamma)^7$Be reaction in halo effective field theory. Eur. Phys. J. A **54**(5), 89 (2018). https://doi.org/10.1140/epja/i2018-12486-5. arXiv:1612.08959
23. J. Vanasse, Fully perturbative calculation of nd scattering to next-to-next-to-leading-order. Phys. Rev. C **88**(4), 044001 (2013). https://doi.org/10.1103/PhysRevC.88.044001. arXiv:1305.0283
24. J. Arvieux, Phase-shift analysis of elastic proton-deuteron scattering cross sections and 3 He excited states. Nucl. Phys. A **221**, 253–268 (1974). https://doi.org/10.1016/0375-9474(74)90317-0
25. A.S. Reiner, On the anomalous effective range expansion for nucleon-deuteron scattering in the $S = 1/2$ state. Phys. Lett. B **28**, 387–390 (1969). https://doi.org/10.1016/0370-2693(69)90327-X
26. A.C. Phillips, G. Barton, Relations between low-energy three nucleon observables. Phys. Lett. B **28**, 378–380 (1969). https://doi.org/10.1016/0370-2693(69)90324-4
27. G. Rupak, A. Vaghani, R. Higa, U. van Kolck, Fate of the neutron-deuteron virtual state as an Efimov level. Phys. Lett. B **791**, 414–419 (2019). https://doi.org/10.1016/j.physletb.2018.08.051. arXiv:1806.01999
28. W.T.H. van Oers, J.D. Seagrave, The neutron–deuteron scattering lengths. Phys. Lett. B **24**, 562–565 (1967). https://doi.org/10.1016/0370-2693(67)90389-9
29. A. Kievsky, M. Gattobigio, Universal nature and finite-range corrections in elastic atom-dimer scattering below the dimer breakup threshold. Phys. Rev. A **87**(5), 052719 (2013). https://doi.org/10.1103/PhysRevA.87.052719. arXiv:1212.3457
30. H.M. Hofmann, G.M. Hale, Microscopic calculation of the He-4 system. Nucl. Phys. A **613**, 69–106 (1997). https://doi.org/10.1016/S0375-9474(96)00418-6. arXiv:nucl-th/9608046
31. H.M. Hofmann, G.M. Hale, He-4 can experiments serve as a database for determining the three-nucleon force? Phys. Rev. C **77**, 044002 (2008). https://doi.org/10.1103/PhysRevC.77.044002. arXiv:nucl-th/0512065,
32. S. König, H.W. Grießhammer, H.W. Hammer, U. van Kolck, Nuclear physics around the unitarity limit. Phys. Rev. Lett. **118**(20), 202501 (2017). https://doi.org/10.1103/PhysRevLett.118.202501. arXiv:1607.04623
33. M. Gattobigio, A. Kievsky, The fate of excited state of ^{4}He. Few Body Syst. **64**(4), 86 (2023). https://doi.org/10.1007/s00601-023-01866-1. arXiv:2305.16814
34. S. Kegel et al., Measurement of the α-particle monopole transition form factor challenges theory: A low-energy puzzle for nuclear forces? Phys. Rev. Lett. **130**(15), 152502 (2023). https://doi.org/10.1103/PhysRevLett.130.152502. arXiv:2112.10582
35. N. Michel, W. Nazarewicz, M. Płoszajczak, Description of the proton-decaying 02+ resonance of the α particle. Phys. Rev. Lett. **131**(24), 242502 (2023). https://doi.org/10.1103/PhysRevLett.131.242502. arXiv:2306.05192
36. U.-G. Meißner, S. Shen, S. Elhatisari, D. Lee, Ab initio calculation of the alpha-particle monopole transition form factor: no puzzle for nuclear forces. Phys. Rev. Lett. **132**(6), 062501 (2024). https://doi.org/10.1103/PhysRevLett.132.062501